Micro-Force measuring apparatus for robotic fish : design, implementation and application

Anquan Liu[1], Jianwei Zhao[2]*, Liang Li[3], Guangming Xie[4]

1. College of Electrical & Information Engineering, Guangxi University of Science & Technology, Liuzhou 545006, China
E-mail: anquanliu186@163.com

2. Center for Research in Mine Robot, School of Mechanical Electronic & Information Engineering, China Univerisity of Mining & Technology, Beijing 100871, China
E-mail: zhaojianwei@cumtb.edu.cn

3. Intelligent Control Laboratory, College of Engineering, Peking University, Beijing 100871, China
E-mail: liatli@pku.edu.cn

4. Intelligent Control Laboratory,College of Engineering, Peking University,Beijing 100871, China
E-mail: xiegming@pku.edu.cn

Abstract: Robotic fish are widely studied for their high propulsive efficiency, maneuverability, speed, acceleration and stealth. Compared to the measurement of the speed and acceleration of robotic fish, the propulsion can hardly be detected because of the micro-force and the movement. In this paper, we designed a micro-force measuring apparatus consisting of a micro-force sensor and a fixing device for robotic fish. The sensor has an accuracy of $0.1mN$ and can transform the force to electronic signal which is convenience to measure. The designed fixing device can limit the lateral movements of robotic fish but have non drag force in the forward swimming direction. Through this apparatus we first measured different propelling models and then compared the propulsion of robotic fish with different shape and stiffness of caudal fins. Robotic fish designed with soft caudal fin can generate maximum propulsion when undulation in the carangiform model.

Key Words: Robotic fish, Micro-force measuring, Trust measurement, Swimming mode, Caudal fin

1 INTRODUCTION

Traditional Autonomous Underwater Vehicle (AUVs) can hardly satisfy the increasing requirements in the propelling efficiency, control of maneuverability, speed, acceleration and stealth. Inspired by natural aquatic creatures, bio-AUVs have shed new light on the contradictions between the devices and the applications. Robotic fish is one of these novel vehicles and has been widely studied and applied.

Previous researches on the robotic fish have mainly on the mechanics of propulsion, speed, acceleration, controllability and maneuverability. In order to uncover the secrecy of why fish swim with high propelling efficiency, Robo-tuna, the first robotic fish in the world, was built in Massachusetts Institute of Technology (MIT) [1]. Through optimization of the geometric of the link length, maximum swimming speed of robotic fish was found in [2]. Cooperative control of multi-robotic fish was investigated for the pushing box task which is impossible finished by single robotic fish [3].

Many researches on the thrust of natural or robotic fish are based on theoretical analysis or computing methods. Lighthill deduced the thrust of fish based on a Elongated Body Theory (EBT) [4]. Thrusts of different body waves can be estimated through this model [5], although the results have a small gap to the experimental examinations. Through computational fluid dynamics (CFD) modeling, thrust of robotic fish can also been assessed [6]. Others compute the average thrusts of fish school based on immersed boundary method to analyze the interactions between fish undulation through assessed thrusts [7].

Researches based on experiments have also been widely studied. Most thrust measurements of robotic fish is based on air bearing which is expensive and inconvenient to be carried out [8, 9]. Luader *et al* [10, 11] built a micro-force detection device based on air bearing and load cell to compare different flapping mode of fins . A micro-force measuring device was designed with a different structure to show the interactions between the active flapping hydrofoils in a side-by-side and tandem formation [12, 13]. In order to find the suitable caudal fin of robotic fish, Park *et al* set up a micro-force apparatus to measure the propulsion of kinds caudal fin with different shapes and stiffness [14].

In this article, we proposed an micro-force measuring apparatus that is cheap and convenient to test for robotic fish. We designed a micro-force measuring system for robotic fish to measure the propulsion with different swimming modes and caudal fins. The measuring system consists of two main parts, micro-force sensor and effective fixing apparatus to limit the lateral movements and relax the for-

*Corresponding author

978-1-4799-7016-2/15/$31.00

ward swimming. The outputs of micro-force sensor are amplified by a differential amplification designed by ourself. Calibration of the whole system was carried out before we applied the system to verify the factors affecting the thrusts of robotic fish. Three swimming mode of thunniform, carangiform and anguilliform are test with the micro-force apparatus [15]. The gaits of each mode is defined according to the corresponding creatures in nature. We find the thunniform acquire the maximum propulsion, and the second is carangiform. Anguilliform results in minmum propulsion. For several fins designed with different shape and stiffness, we found it is soft fan-shaped fin caudal fin that generate the maximum thrust with the same undulation mode [14]. These results corresponds the natural fish observed by biologists [16, 17].

The remainder of the paper is organized as follows. In Section II, we present the prototype of a carangiform robotic fish. Then design and implementation the micro-force measuring are given in Section III. The fixing apparatus is introduced in section IV In Section V, we apply our micro-force measuring system to verify the thrusts of different shape and stiffness caudal fins. We also compare the relationship between the propulsion and the swimming modes of robotic fish in section6 The results and discussions conclude our work in Section VII.

2 Prototype of Robotic Fish

The prototype of robotic fish we used in these experiments is made in our laboratory according to carangiform fish [18, 19]. It consists of three parts, a rigid head, a flexible body and a caudal fin see Fig. 1. The rigid head is designed with a streamline shape and contains the battery, control module and wireless communication module. The flexible body is made of soft rubber and three links controlled by three servomotors are fixed inside of the skin. The caudal fin are designed with gradually varied stiffness that is similar to the real one. The robotic fish is propelled through body undulation resembling to the natural fish. The swimming mode is controlled by the microcontroller inside the robotic fish. In addition, the form of undulation mimics the real gaits observed in the real one.

The robotic fish body form a nature Cartesian coordinate system, and we place the nose of fish at the origin. Just like real fish, robotic fish propel itself by the active undulation of flexible body. And the function of the body wave is defined as [5]

$$z = (c_1(x-x_0)^2 + c_2(x-x_0))\sin(kx+2\pi ft) \qquad (1)$$

where x is the displacement along the boy axis and z is the transverse displacement of body, c_1 and c_2 are linear and quadratic wave amplitude envelope, k denotes the number body wave. f is the frequency of body wave. x_0 is defined as fixed point which means this point has no oscillation in z axis. Different parameters represent different undulation of the flexible body, and here we reference the locomotion of real carangiform fish described in [20, 21]. The pattern of body undulation is shown in Fig. 1 (b), and robotic fish is controlled by CPG controller in a discrete form [22]. The detail implementation process can be referred in our previous work [23].

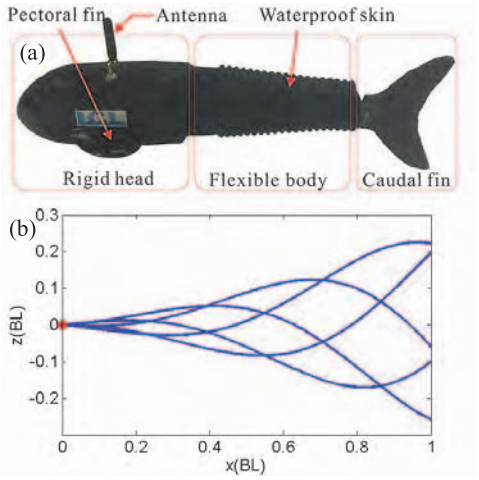

Figure 1: Robotic fish prototype and undulation body wave. (a) Robotic fish consisting of rigid head, flexible body and caudal fin. (b) Cluster of body undulation for robotic fish based on carangifrom fish.

3 Micro-force Measuring Apparatus

In this section, we introduce the micro-force apparatus in detail. The micro-force sensor is first introduced. As the output of the sensor is very small that we need a amplification, we then present the simple amplification circuit designed for the micro-force sensor and the method of data acquisition. Before the experiments of testing thrusts of robotic fish, we also present the calibration of our micro-force measuring system. In order to test the propulsion of robotic fish, we also give a machine construction of fixing the robotic fish.

3.1 Micro-force Sensor

We choose HBM Z6FC3 as the micro-force sensor to detect the thrust of robotic fish on time (see the apparatus in Fig. 5). The accuracy of the load cell is $0.1mN$ that is satisfy to our test requirement. The principle of the micro-force detection is base on the deformation of the sensor unit, and the signal of physical deformation is transformed to electronic signal with differential amplification. Since the force that can be detect is only in the direction of deformation, the tangential force have none effect of the test. Therefore, the tangential forces that are generated by the undulation will be eliminated by the micro-force sensor. Differential Amplification is widely applied in the systems of micro variables with noise suppression. However, as the force we need to test is so tiny that the transformed electronic signal is still very small. And it can hardly be acquired by usual data acquisition device without signal amplification.

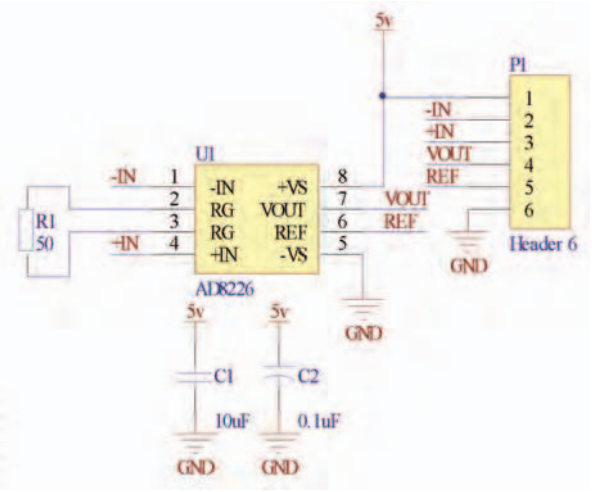

Figure 2: Principle of signal amplification

3.2 Signal Amplification

We used AD8226, a differential amplifier chip, to amplify the output signal of the micro-force sensor. The principle of the amplification is designed as shown in Fig. 2, where the resistance of R_1 determines the amplification times for the signal input. The detail transform function is defined as [24]

$$G = 1 + \frac{49.4k\Omega}{R_G} \tag{2}$$

Where R_G is R_1 and the amplification factor G can be accessed whenever given a resistance value of R_1. Here, we chose R_1 with 50Ω, thus the amplification of this circuit is around 989.

After this amplification, we get the output voltage through National Instruments (NI) 6210 data acquisition card with accuracy of 2.69 mV Voltage is acquired with a sampling rate of 5000 and each test lasts 10 s. In order to suppress noise of the system, we test five groups of data for each test point. The voltage of the test point is regarded as the average of these five test groups. A snapshot of the device of the signal amplification and current acquisition card is shown in Fig. 3(a). One typical measuring amplification signal is shown in Fig. 3(a), the oscillation of the data corresponds to the undulation of the robotic fish. The frequency of the voltage is twice that of fish body wave, which is because the force we tested has no direction and the robotic fish undulate symmetrically. The undulation of right is the same to that of left.

3.3 Measurement Calibration

The calibration of the sensor is carried out after the signal amplification of voltage output. We first test the voltage outputs without any force on the sensor with five times, and each lasts 10 s. With a series of hook weights to press

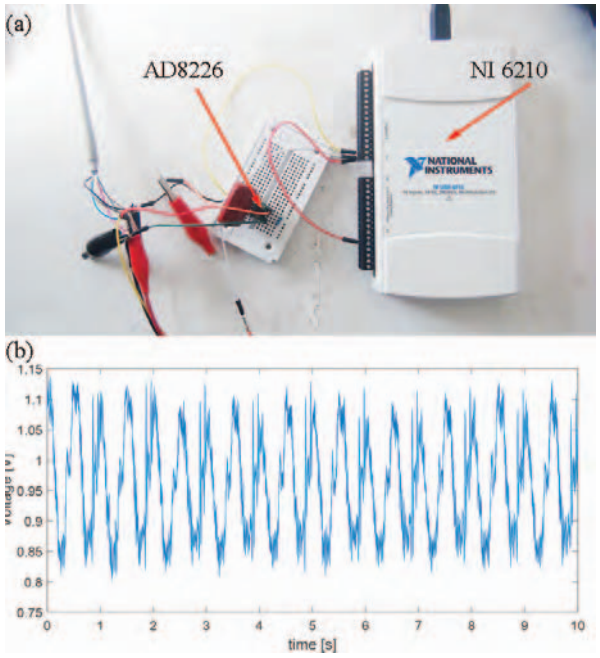

Figure 3: Amplification circuit and one test case. (a) Snapshot of the circuit of amplification. (b) Voltage of time within 10s. The frequency of undulation of force tested is twice of that of robotic fish body wave. Here, the propulsion parameters are defined as frequency 1.0, amplitude of the first joint 12^o, amplitude of the second joint 22, amplitude of the third joint 27, phase difference between joint one and joint two 0.678 and phase difference between joint one and three.

the sensor, we test five group data for each pressure. The calibration results of our system are shown in Fig. 4. The transform function of forcing (F) of output voltage (V) is fitted as a linear system $F = k \cdot V - b$ The parameters k and b are identified through Least Squares, and the function is

$$F = 9.9985V - 10.36 \tag{3}$$

The summed square of residuals (SSE) is 3.217×10^{-6}. R-Square, representing the correlation between the response values and the predicted response value, is 1. Adjusted R-Square is also 1. Root Mean Squared Error (RMSE), estimating of the standard deviation of the random component in the data, reaches 5.978×10^{-4}. Through these indexes, we can find this fitting results is confident.

4 Fixing Apparatus

Fish should overcome the drag force by forward propulsion when fish swims steady. Thus, faster speed corresponds to larger thrust, as the drag is proportional to the square of speed. However, its hard to measure the thrust when fish swim forward in the water. We designed a fixing apparatus to detect the thrusts of robotic fish by fixing the robotic fish in the water. The fixing apparatus can limit the lateral movements of robotic fish but have none drag in the

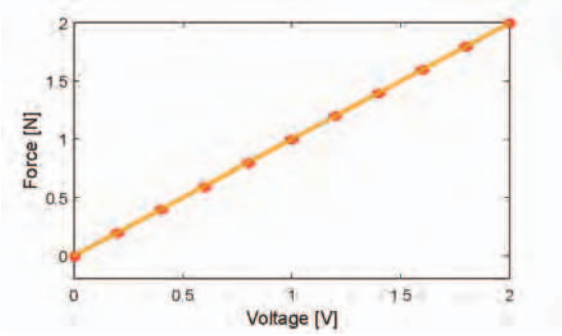

Figure 4: The calibration of our system. we chose five standard weights to calibrate our micro-force sensor. The read markers represent the discrete test points. And the orange line denotes the fitted curve based on the calibration points.

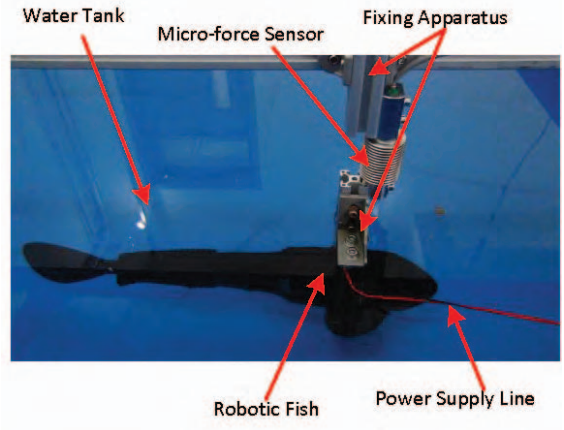

Figure 5: Experimental apparatus combining robotic fish, fixing apparatus and micro-force sensor

direction of forward propulsion, because the thrusts in the swimming direction lead fish swim forward.

The structure of our apparatus is shown in Fig. 5, where the fixing apparatus is applied in the thrusts test with a robotic fish in the water tank. The fixing apparatus connecting the self of the tank and our robotic fish. And the deformation of the micro-force sensor is fixed in the same direction that the robotic fish swims forward. The lateral oscillation force is perpendicular to the direction of test force, thus having none effects on the propulsion test even though the robotic fish get an lateral oscillation.

5 Application Studies

In order to test and verify the effectiveness of our micro-force measuring apparatus, we designed two simple experiments. We first test the thrusts of different swimming mode of anguilliform, carangiform and thunniform swimming, and the comparison among them has also been given. We then compared the thrusts of different shape and stiffness of caudal fins with several oscillating frequencies.

Table 1: Control parameters

Swimming mode	thunniform	carangiform	anguilliform
Frequency [Hz]	1.2	1.0	0.4
Amplitude of 1st joint [^{o}]	0	12	40
Amplitude of 2nd joint [^{o}]	35	22	40
Amplitude of 3rd joint [^{o}]	35	27	40
Phase difference between 1st and 2nd joint	0	0.698	2.0
Phase difference between 1st and 3rd joint	0	2.513	3.0

5.1 Trusts of Different Swimming Mode

We test three swimming modes of fish in nature, anguilliform swimming, carangiform swimming and thunniform swimming [25]. For anguilliform swimming mode, fish swims with large amplitude but small frequency. And carangiform fish swims by the undulation of the two-third of the rear body with gentle amplitude and frequency. But fish swim in the thunniform will have higher frequency and smaller amplitude of the one-third rear body. We choose three typical swimming mode according to natural fish described in [26], and the control parameters for our robotic fish are presented in table in detail in Tab. 1. The control parameters are chosen based on the natural body wave and discrete for the three joints. Based on our previous work on the locomotion controller and its implementation, we can directly send the control parameters to the robotic fish [22, 23]. Each form tested five times to inhibit the environment noise. And the average of these five tests is regarded as the final thrust. Thrusts of these three swimming modes is 0.784 N, 0.668 N, 0.292 N, respectively. The standard deviation of five tests are 0.0205, 0.0237, 0.173.

The thrusts of these three typical swimming modes are shown in Fig. 6. These test results are similar to the nature observations [27]. The same as the nature fish, the swimming mode that generates the maximum thrust is thunniform. Therefore, this swimming mode is quite suitable to cruising, such as tuna. Anguiliform swimming mode results in minimum propulsion and thus swim with low speed.

5.2 Trusts of Shape and Stiffness of Caudal Fin

The caudal fins are divided into two groups with different shapes, fan-shaped tails and lunate caudal fins. The detail fin properties are show in Table 2. And for each shape, two different stiffness are included, soft and rigid. The stiffness is changed by adding some carbon rods in the soft caudal fins. Therefore, we can not only compare the thrusts of different stiffness of caudal fin in the same shape but also compare different shapes of caudal fin in the same stiffness. Fig. 7 shows the thrusts of different shape and stiffness fin-

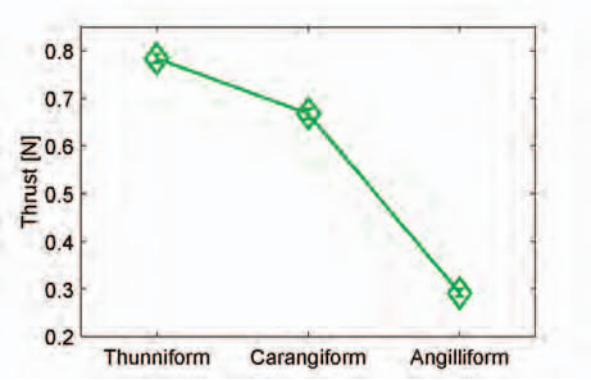

Figure 6: Thrust vs. swimming mode. Three different swimming modes have been tested. Thunniform, Carangiform, Anguilliform swimming mode generate thrusts of 0.784 N, 0.668 N, 0.292 N, respectively.

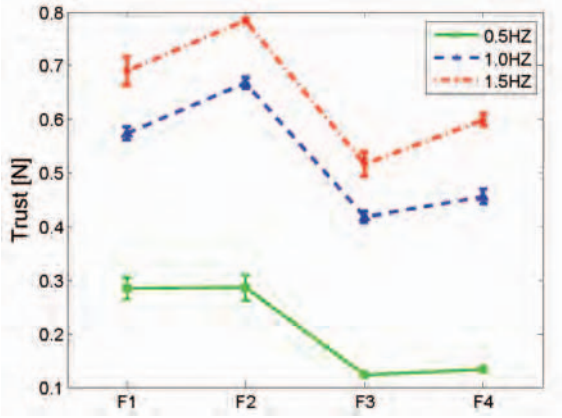

Figure 7: Trust vs. caudal fin of differential shape and stiffness.

Table 2: Caudal Fin Properties

ID	F1	F2	F3	F4
Shapes				
Chord Length [cm]	14	14	12.8	12.8
Aspect Ratio	1.97	1.97	2.42	2.42
Shape	Fan-shaped	Fan-shaped	Lunate	Lunate
Stiffness	rigid	soft	rigid	soft

s under the same body undulation with three frequencys. Four different caudal fins are labeled in the x axis (see the details in Table 2) and the y axis represents the thrust generated by the corresponding caudal fin with the same control parameters. The same as the last experiment, we also test five times of the thrusts. Each test lasts 10 s and thus generates 50000 data.

Similar to the most previous researches on the thrust of caudal fin, thrust of the fin and body wave increases with the frequency increases. But the speed of the increasing decreases with increasing frequency. From the comparison of the shape, we can find robotic fish equipped with soft-fan-shaped caudal fin gets larger thrust. While the softer fin can acquire larger thrust than the harder caudal fins. In conclusion, soft fan-shaped fin benefits the propulsion of robotic fish.

According to the observations of natural fish, most fish evolute with soft caudal fins with high propulsion. However, few fish have fan-shaped caudal fins, one of the explanation may be that lunate caudal fin has higher St thus has peak propelling efficiency [28]. For man-made underwater vehicles, we can acquire higher propulsion with fan-shaped caudal fin.

6 Discussion and Conclusion

We designed an cheaper and convenient apparatus to test the thrust of robotic fish that is very small and uneasy to be detected steady. The apparatus consists of two main parts, the micro-force sensor and the fixing device. For the micro-force sensor, an amplification circuit is also designed. With this sensor and circuit we can measure the tiny force of 0.1 mN. As robotic fish is propelled by body undulation, the force both in the forward and lateral will be generated. And these two direction force is always coupled. Therefore we designed a simple fixing apparatus that can decouple these two direction forces and measure only the force in the forward direction. In order to verify the effectiveness of our apparatus, we applied this device to measure the thrusts of robotic fish with different caudal fins and swimming modes. The detection of the thrust is similar to the previous results.

Compare to the test results of previous works, we get the thrust in the order of 100 mN, which is the same with the propulsion of other experiments [8, 10, 11, 17]. These experiments are based on air bearing with complex setup and test steps. With our simple apparatus, thrusts of robotic fish can also be accessed. There are also many aspects to improve our device, such as reducing the length between the micro-force sensor test point and the robotic fish to access the thrusts force.

From the measurement of the thrusts of three swimming mode, we find the thunniform swimming mode generate the maximum propulsion. This is may help us understand why the creatures with high speed and acceleration swim with this mode [27]. The verifying experiments on the effects of caudal fin to propulsion have not only proofed the effectiveness of our apparatus but also point out the relationship between the propulsions and the caudal fins. With fan-shaped soft caudal fin, maximum propulsion will be generated, but the propulsion efficiency is lower than soft lunate caudal fin. This may indicate that natural fish trade off both propulsion and the efficiency and thus soft lunate

caudal fin are evolved in the final.

In the future, we can apply this measurement to other meaningful experiments on the thrusts. A detail and systematic studies on the relationship between the thrusts and caudal fins will be carried out to find the suitable fin considering the shape and stiffness. Therefore, we can optimize the speed of robotic fish with the caudal fin. Also, the thrusts of fish school can be tested with multi-micro-force sensors, therefore, the transformation of propulsion between fish school can be detected. This may give an explanation for why do fish school in the hydrodynamics aspect.

REFERENCES

[1] M. S. Triantafyllou and G. S. Triantafyllou, "An efficient swimming machine," *Scientific American*, vol. 272, no. 3, pp. 64–70, 1995.

[2] J. Yu, L. Wang, and M. Tan, "Geometric optimization of relative link lengths for biomimetic robotic fish," *IEEE Transactions on Robotics*, vol. 23, no. 2, pp. 382–386, 2007.

[3] d. Zhang, L. Wang, J. Yu, and M. Tan, "Coordinated transport by multiple biomimetic robotic fish in underwater environment," *IEEE Transactions on Control Systems Technology*, vol. 15, no. 4, pp. 658–671, 2007.

[4] M. J. Lighthill, "Note on the swimming of slender fish," *Journal of Fluid Mechanics*, vol. 9, no. 02, pp. 305–317, 1960.

[5] L. Li, C. Wang, and G. Xie, "Modeling of a carangiform-like robotic fish for both forward and backward swimming: Based on the fixed point," in *2014 IEEE International Conference on Robotics and Automation (ICRA)*, 2014, pp. 800–805.

[6] A. Mart, Z. Chen, K. Maarja, and X. Tan, "Analytical and computational modeling of robotic fish propelled by soft actuation material-based active joints," in *The 2009 IEEE/RSJ International Conference on Intelligent Robots and Systems*, 2009, pp. 2126–2131.

[7] X. Zhu, G. He, and X. Zhang, "Flow-mediated interactions between two self-propelled flapping filaments in tandem configuration," *Physical Review Letters*, vol. 113, no. 23, p. 238105, 2014.

[8] J. L. Tangorra, G. V. Lauder, I. W. Hunter, R. Mittal, P. G. A. Madden, and M. Bozkurttas, "The effect of fin ray flexural rigidity on the propulsive forces generated by a biorobotic fish pectoral fin," *Journal of Experimental Biology*, vol. 213, no. 23, pp. 4043–4054, 2010.

[9] J. H. J. Buchholz, R. P. Clark, and A. J. Smits, "Thrust performance of unsteady propulsors using a novel measurement system, and corresponding wake patterns," *Experiments in Fluids*, vol. 45, no. 3, pp. 461–472, 2008.

[10] C. J. Esposito, J. L. Tangorra, B. E. Flammang, and G. V. Lauder, "A robotic fish caudal fin: effects of stiffness and motor program on locomotor performance," *Journal of Experimental Biology*, vol. 215, no. 1, pp. 56–67, 2012.

[11] J. Tangorra, C. Phelan, C. Esposito, and G. Lauder, "Use of biorobotic models of highly deformable fins for studying the mechanics and control of fin forces in fishes," *Integrative and Comparative Biology*, 2011.

[12] P. A. Dewey, D. B. Quinn, B. M. Boschitsch, and A. J. Smits, "Propulsive performance of unsteady tandem hydrofoils in a side-by-side configuration," *Physics of Fluids (1994-present)*, vol. 26, no. 4, pp. 041 903–041 918, 2014.

[13] B. M. Boschitsch, P. A. Dewey, and A. J. Smits, "Propulsive performance of unsteady tandem hydrofoils in an in-line configuration," *Physics of Fluids (1994-present)*, vol. 26, no. 5, pp. 051 901–051 917, 2014.

[14] Y. J. Park, U. Jeong, J. Lee, S. R. Kwon, H. Y. Kim, and K. J. Cho, "Kinematic condition for maximizing the thrust of a robotic fish using a compliant caudal fin," *IEEE Transactions on Robotics*, vol. 28, no. 6, pp. 1216–1227, 2012.

[15] E. D. Tytell, I. Borazjani, F. Sotiropoulos, T. V. Baker, E. J. Anderson, and G. V. Lauder, "Disentangling the functional roles of morphology and motion in the swimming of fish," *Integrative and Comparative Biology*, vol. 50, no. 6, pp. 1140–1154, 2010.

[16] J. F. Peng, J. O. Dabiri, P. G. Madden, and G. V. Lauder, "Non-invasive measurement of instantaneous forces during aquatic locomotion: a case study of the bluegill sunfish pectoral fin," *Journal of Experimental Biology*, vol. 210, no. 4, pp. 685–698, 2007.

[17] G. V. Lauder, E. J. Anderson, J. Tangorra, and P. G. A. Madden, "Fish biorobotics: kinematics and hydrodynamics of self-propulsion," *Journal of Experimental Biology*, vol. 210, no. 16, pp. 2767–2780, 2007.

[18] J. Shao, L. Wang, and J. Yu, "Development of multiple robotic fish cooperation platform," *International Journal of Systems Science*, vol. 38, no. 3, pp. 257–268, 2007.

[19] ——, "Development of an artificial fish-like robot and its application in cooperative transportation," *Control Engineering Practice*, vol. 16, no. 5, pp. 569–584, 2008.

[20] J. J. Videler and F. Hess, "Fast continous swimming of two pelagic predators, saithe (pollachius-virens) and mackerel (scomber-scombrus)-a kinematic analysis," *Journal of Experimental Biology*, vol. 109, no. MAR, pp. 209–228, 1984.

[21] C. S. Wardle, J. J. Videler, and J. D. Altringham, "Tuning in to fish swimming waves-body form, swimming mode and muscle function," *Journal of Experimental Biology*, vol. 198, no. 8, pp. 1629–1636, 1995.

[22] C. Wang, G. Xie, L. Wang, and M. Cao, "Cpg-based locomotion control of a robotic fish: Using linear oscillators and reducing control parameters via pso," *International Journal of Innovative Computing Information and Control*, vol. 7, no. 7B, pp. 4237–4249, 2011.

[23] L. Li, C. Wang, G. Xie, and H. Shi, "Digital implementation of cpg controller in avr system," in *Proceedings of the 33rd Chinese Control Conference*, 2014, pp. 8293–8298.

[24] Analog Devices, DataSheet AD8226, http://www.analog.com/static/imported-files/data_sheets/AD8226.pdf.

[25] L. D. M. Sfakiotakis, M. and J. B. C. Davies, "Review of fish swimming modes for aquatic locomotion," *IEEE Journal of Oceanic Engineering*, vol. 24, no. 2, pp. 237–252, 1999.

[26] J. Videler, *Fish Swimming*. London: Chapman & Hall, 1993.

[27] P. W. Webb, "Form and function in fish swimming," *Scientific American*, vol. 251, no. 1, pp. 72–82, 1984.

[28] M. S. Triantafyllou, F. S. Hover, A. H. Techet, and D. K. Yue, "Review of hydrodynamic scaling laws in aquatic locomotion and fishlike swimming," *Applied Mechanics Reviews*, vol. 58, no. 4, pp. 226–237, 2005.